

# Characterization of Airborne Fibers via Fraunhofer Theory: Examination of the Validity of Fraunhofer Theory Using the Exact Scattering Theory MMP

Henning Sagehorn\*, Joachim List\*\*, Till Wiegand\*\*\*, Reiner Weichert\*\*, Thomas Wriedt\*\*\*

(Received: 6 March 2001)

## Abstract

Owing to the health hazard of respirable airborne fibers, there is great interest in detectors able to monitor fibers on-line. This paper features such an optical fiber detector which is based on Fraunhofer theory for the estimation of fiber size. Because Fraunhofer theory is not an exact theory and does not take into account the three-dimensional shape of fibers and their material properties, comparative com-

putations with an exact theory, the multiple multipole method (MMP), a variant of the generalized multipole technique, were performed. For small fiber diameters these simulations showed differences between diffraction patterns calculated via Fraunhofer theory and scattering patterns computed with MMP. The differences were strongly dependent on the optical properties of the fiber material.

## 1 Introduction

Nowadays fibrous particles are widely used, especially as insulating materials in buildings. Owing to corrosion these fibers may become airborne. Other sources of airborne fibers include natural sources (volcanic eruptions, forest fires, weathering of stones, etc.), iron smelting and combustion of coal (in coal-fired power plants, domestic stoves, etc.). Airborne fibers are considered to cause serious health hazards, depending on their material and geometric properties. According to the World Health Organization (WHO), fibers are classified as hazardous, if they have lengths of more than 5  $\mu\text{m}$ , diameters of less than 3  $\mu\text{m}$  and length to diameter ratios of more than 3:1. In this case fibers are considered respirable and may cause serious lung diseases such as cancer [1].

The standard procedure for the detection of respirable fibers is described in the German guideline VDI 3492 [2]. It is based on collecting airborne fibers on a filter and classifying them under a scanning electron microscope with the human eye. This procedure is, of course, laborious and

expensive as trained personnel have to detect the fibers and differentiate between harmful and harmless ones, making it a very time-consuming method. Accuracy is another problem, as was found by Höfert et al. [3, 4]. Sending one probe to different laboratories for estimation of fiber concentration led to very different results, and even the reference estimations done by four laboratories showed differences in fiber concentration of up to 40%.

Because of the drawbacks of scanning electron microscopy, extensive research is under way to develop new fiber detection methods. The most promising ones seem to be a wide variety of light scattering methods, as they have the advantage of delivering fiber geometries in a fairly short time. These methods have in common that airborne fibers are illuminated by a laser beam while their scattered light is recorded with some sort of detector. There are several ways to realize such setups. Baron [5] and Kaye [6] gave an overview of the most common optical fiber detectors in review articles. Most detectors considered there do not characterize fibers according to their length and diameter, so differentiation between harmful and harmless ones is not necessarily possible. Kaye introduced a fiber detector able to characterize the fiber shape via a neural network [6], but the extension to characterize the fiber size has not yet been done.

As part of a German research program for improvement of fiber detection methods [1], Barthel et al. [7] developed a

\* Dipl.-Phys. H. Sagehorn, Universität Bremen, Badgasteiner Str. 3, 28359 Bremen (Germany). E-mail: sage@iwt.uni-bremen.de

\*\* Dipl.-Phys. J. List, Prof. Dr.-Ing. R. Weichert, Technische Universität Clausthal, Leibnizstr. 19, 38678 Clausthal-Zellerfeld (Germany).

\*\*\* T. Wiegand, Dr.-Ing. T. Wriedt, Institut für Werkstofftechnik, Badgasteiner Str. 3, 28359 Bremen (Germany).

device which is able to detect the scattering profile of a particle over the azimuthal scattering angle. Detectors being aligned over the same scattering but different azimuthal angles each record the same intensity if a sphere is detected but different intensities for a fiber. The standard intensity deviation of the detectors depends on the length to diameter ratio, and the total intensity of all detectors on the fiber size. This method has the advantage of estimating the fiber properties on-line.

Yet another on-line fiber detector was developed at the University of Clausthal. It is based on Fraunhofer diffraction to estimate the fiber geometry on-line [8]. A particle in a laser beam generates a characteristic scattering profile. Evaluation of this profile using Fraunhofer diffraction gives information about the fiber geometries.

Fraunhofer diffraction is widely used to characterize particles of large size relative to the wave-length of the incident light and is considered to give valid results for these particles. Development of a fiber detector as done in this project leads to the necessity of characterizing respirable fibers where the Fraunhofer theory may no longer be valid. Thus an extensive investigation has been carried out comparing Fraunhofer theory with an exact theory. There are various exact theories available for such an investigation [9].

The discrete dipole approximation (DDA) is often applied to scattering by fibers [10], but because volume discretization is used, the computational demands are very high.

For our applications we chose the multiple multipole method (MMP) [11], which is a variant of the generalized multipole theory (GMT) [12]. This method has already been tested on various particle shapes by *Comberg* and *Wriedt* [13].

## 2 Description of the Fiber Detector

The setup of the detection unit of the device developed at the University of Clausthal is shown in Figure 1. The detection system features a pulsed Nd:YAG laser beam illuminating the fiber in the measurement volume. The scattered light is recorded by a CCD camera after separating the unscattered beam from the scattered light. If a fiber is oriented parallel to the beam in the measurement volume, the fiber top would be lit, resulting in a scattering profile similar to that of a sphere. Therefore, a second identical setup perpendicular to the first one is used. Its laser beam then lights the fiber perpendicular to its axis. The influence of both setups on each other is negligible, as only a small amount of light is scattered on to the CCD detector of the other setup.

The scattering profile of a detected fiber, which is assumed to have a cylindrical shape, is analyzed by an algorithm. The algorithm estimates the fiber orientation relative to the incoming laser beam and finds intensity minima allowing calculation of the fiber geometries via Fraunhofer theory. In

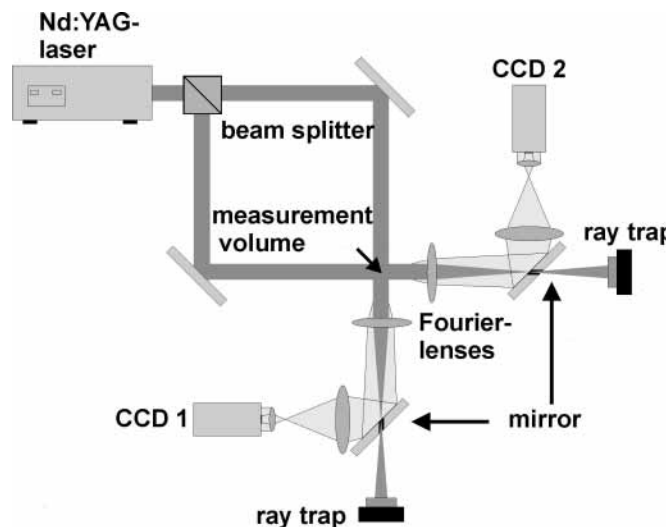


Fig. 1: Setup of the fiber detector developed at the University of Clausthal.

Fraunhofer theory the fiber diameter is inversely proportional to the distance of minima positions. Usually the distance of neighboring minima or the position of the first-order minimum are chosen for fiber diameter estimation. The fiber geometry can also be computed from the position of the half-width of the zeroth-order maximum, if the minima cannot be distinguished.

The detector itself was tested with glass fibers having lengths of 5–50  $\mu\text{m}$  and diameters of 2.6–20  $\mu\text{m}$ . The measurement errors were found by collecting the previously detected fibers and characterizing them by scanning electron microscopy. The error in fiber size estimation was found to be about 10% for fiber axis orientation perpendicular to the laser beam and up to 30% for length estimation of tilted fibers.

Unfortunately, Fraunhofer theory used for fiber size estimation has several drawbacks. The fiber is approximated by rectangles corresponding to the geometry of the fiber projection because the theory is valid only for two-dimensional objects. Another is that the optical properties of the fiber material are not taken into account and the fiber is assumed to be opaque. Finally, Fraunhofer theory is valid only for objects large compared with the wavelength of the illuminating laser beam. As airborne respirable fibers usually do not fulfill these requirements, there could be an error in fiber size estimation.

Hence although the fiber detector shows good results for large fibers, the ability to estimate fiber geometries of small WHO fibers has to be investigated. Therefore, comparative light scattering simulations have to be done to show the validity of estimating the fiber size using Fraunhofer diffraction analysis. Thus scattering profiles computed by Fraunhofer diffraction were compared with profiles of fibers simulated with the MMP.

### 3 Introduction to MMP

The MMP is one of the powerful numerical methods called generalized multipole techniques (GMT). The state of the art GMT was reviewed in an edited volume [12] published recently. MMP was developed by *Hafner* and *Bomholt* [11] for general electromagnetic computations. It is a semianalytical method, in the sense that the electromagnetic fields are expressed as a linear combination of multiple multipoles, whereas the amplitudes of the multipoles are obtained by enforcing the boundary conditions in a set of matching points.

The scattering of electromagnetic waves by a dielectric particle ( $D_i$ ) with a boundary  $S$  and exterior  $D_s$  may be formulated in terms of the following boundary value problem: given  $\mathbf{E}_0, \mathbf{H}_0$  in  $D_s$  as an entire solution for the Maxwell equations, find the scattered electromagnetic field  $\mathbf{E}_s, \mathbf{H}_s$  in  $D_s$  and the internal electromagnetic fields  $\mathbf{E}_i, \mathbf{H}_i$  in  $D_i$  satisfying the Maxwell equations

$$\begin{aligned}\nabla \times \mathbf{E}_t - jk_0 \mu_t \mathbf{H}_t &= 0 \\ \nabla \times \mathbf{H}_t - jk_0 \varepsilon_t \mathbf{E}_t &= 0\end{aligned}\quad (1)$$

and the boundary condition at the interface

$$\begin{aligned}\mathbf{n} \times \mathbf{E}_i - \mathbf{n} \times \mathbf{E}_s - \mathbf{n} \times \mathbf{E}_0 &= 0 \\ \mathbf{n} \times \mathbf{H}_i - \mathbf{n} \times \mathbf{H}_s - \mathbf{n} \times \mathbf{H}_0 &= 0.\end{aligned}\quad (2)$$

The scattered field  $\mathbf{E}_s, \mathbf{H}_s$  additionally has to fulfill the Silver Müller radiation condition at infinity:

$$\frac{\mathbf{x}}{|\mathbf{x}|} \times \sqrt{\mu_s} \mathbf{H}_s + \sqrt{\varepsilon_s} \mathbf{E}_s = o\left(\frac{1}{|\mathbf{x}|}\right), \quad (3)$$

as  $|\mathbf{x}| \rightarrow \infty$ , uniformly for all directions  $\mathbf{x}/|\mathbf{x}|$ . Index  $t$  is defined as  $t = s, i$ ;  $\mu_t$  and  $\varepsilon_t$  are the permeability and the permittivity of domain  $D_t$ , respectively,  $k_0$  denotes the wavenumber in  $D_s$  and  $\mathbf{n}$  is the unit outward normal vector on  $S$ .

An approximate solution  $\mathbf{E}_t^N, \mathbf{H}_t^N$  of the scattering problem is constructed as a finite linear combination of fields of multiple multipoles having different origins. For the scattered field these multipoles will be located inside  $D_i$ , so that  $\mathbf{E}_s^N, \mathbf{H}_s^N$  is a radiating solution to the Maxwell equations being regular in  $D_s$ . For the internal field  $\mathbf{E}_i^N, \mathbf{H}_i^N$  the radiating multipoles will be located in  $D_s$ , while the regular ones are located in  $D_i$ . The origins of the multipoles are distributed according to the shape of the domain.

It can be shown [14] that the following estimate holds for the approximate solution:

$$\begin{aligned}\|\mathbf{E}_s - \mathbf{E}_s^N\|_{\infty, G_s} + \|\mathbf{H}_s - \mathbf{H}_s^N\|_{\infty, G_s} + \|\mathbf{E}_i - \mathbf{E}_i^N\|_{\infty, G_i} \\ + \|\mathbf{H}_i - \mathbf{H}_i^N\|_{\infty, G_i} \\ \leq C(\|\mathbf{n} \times \mathbf{E}_s^N + \mathbf{n} \times \mathbf{E}_0 - \mathbf{n} \times \mathbf{E}_i^N\|_{2, S} \\ + \|\mathbf{n} \times \mathbf{H}_s^N + \mathbf{n} \times \mathbf{H}_0 - \mathbf{n} \times \mathbf{H}_i^N\|_{2, S})\end{aligned}\quad (4)$$

where  $G_s \subset D_s$ ,  $G_i \subset D_i$  and  $C$  is a constant depending on  $G_t$  and  $S$ .

According to the above estimate, a quasi-solution to the boundary value condition can be obtained by approximating the tangential components of the incident fields  $\mathbf{E}_0, \mathbf{H}_0$  on the boundary of the scatterer by multiple multipoles. For estimate (4) to be valid the system of multiple multipoles is required to be complete, which has been proved by *Wriedt* et al. [14].

The implementation of MMP into a numerical algorithm for calculation of the fields of a dielectric scatterer is done the following way. Let

$$\begin{aligned}\mathcal{M}_{mnp}^{3t} &= \mathbf{M}_{mn}^{3t}[k_t(\mathbf{x} - \mathbf{x}_{0p})] \\ \mathcal{N}_{mnp}^{3t} &= \mathbf{N}_{mn}^{3t}[k_t(\mathbf{x} - \mathbf{x}_{0p})]\end{aligned}\quad (5)$$

be the radiating spherical vector wavefunctions with their singularities located at  $\mathbf{x}_{0p}$  such that the system  $\{\mathbf{n} \times \mathcal{M}_{mnp}^{3t}, \mathbf{n} \times \mathcal{N}_{mnp}^{3t}\}$  is linearly independent and complete on  $S$ .  $\{\mathcal{M}_{mnp}^{3t}, \mathcal{N}_{mnp}^{3t}\}$  of course fulfill the Maxwell equations. Index  $p$  denotes the number of the multipole,  $k_t = k_0 \sqrt{\varepsilon_t \mu_t}$  is the wavenumber of the domain  $D_t$  and  $\mathbf{M}_{mn}^{3t}$  and  $\mathbf{N}_{mn}^{3t}$  are defined as

$$\begin{aligned}\mathbf{M}_{mn}^{3t} &= h_n(k_t r) \left[ jm \frac{P_n^{(m)}(\cos \theta)}{\sin \theta} \mathbf{e}_\theta - \frac{dP_n^{(m)}(\cos \theta)}{d\theta} \mathbf{e}_\varphi \right] e^{jm\varphi} \\ \mathbf{N}_{mn}^{3t} &= \left\{ \begin{aligned} &n(n+1) \frac{h_n(k_t r)}{k_t r} P_n^{(m)}(\cos \theta) \mathbf{e}_r \\ &+ \frac{[k_t r h_n(k_t r)]'}{k_t r} \left[ \frac{dP_n^{(m)}(\cos \theta)}{d\theta} \mathbf{e}_\theta + jm \frac{P_n^{(m)}(\cos \theta)}{\sin \theta} \mathbf{e}_\varphi \right] \end{aligned} \right\} e^{jm\varphi}\end{aligned}\quad (6)$$

where  $(\mathbf{e}_r, \mathbf{e}_\varphi, \mathbf{e}_\theta)$  are the unit vectors in spherical coordinates,  $n$  is the order of the multipole,  $m$  is the azimuthal mode,  $h_n$  denotes the Hankel function and  $P_n^{(m)}$  are the Legendre polynomials.

The approximate internal and scattered electric fields  $\mathbf{E}_t^N$  are represented as a linear combination of radiating spherical vector wavefunctions with  $P$  different poles:

$$\mathbf{E}_s^N = \sum_{p=1}^P \sum_{n=1}^{N_p} \sum_{m=-n}^n a_{mnp}^N \mathcal{M}_{mnp}^{3s} + b_{mnp}^N \mathcal{N}_{mnp}^{3s} \quad (7)$$

$$\mathbf{E}_i^N = \sum_{p=1}^P \sum_{n=1}^{N_p} \sum_{m=-n}^n c_{mnp}^N \mathcal{M}_{mnp}^{3i} + d_{mnp}^N \mathcal{N}_{mnp}^{3i}. \quad (8)$$

The expansion coefficients  $a_{mnp}^N, b_{mnp}^N, c_{mnp}^N$  and  $d_{mnp}^N$  will be obtained by minimizing the residual field:

$$\begin{aligned}\mathbf{a} = \arg \min \{ \|\mathbf{n} \times \mathbf{E}_s^N + \mathbf{n} \times \mathbf{E}_0 - \mathbf{n} \times \mathbf{E}_i^N\|_{2, S}^2 \\ + \|\mathbf{n} \times \mathbf{H}_s^N + \mathbf{n} \times \mathbf{H}_0 - \mathbf{n} \times \mathbf{H}_i^N\|_{2, S}^2 \}\end{aligned}\quad (9)$$

where

$$\mathbf{a}^T = [a_{mnp}^N, b_{mnp}^N, c_{mnp}^N, d_{mnp}^N].$$

While the approximate solution  $\mathbf{E}_t^N$ ,  $\mathbf{H}_t^N$  converges to the exact solution  $\mathbf{E}_t$ ,  $\mathbf{H}_t$ , the relative error may be evaluated by

$$\varepsilon_N = \frac{\|\mathbf{n} \times \mathbf{E}_s^N + \mathbf{n} \times \mathbf{E}_0 - \mathbf{n} \times \mathbf{E}_i^N\|_{2,S} + \|\mathbf{n} \times \mathbf{H}_s^N + \mathbf{n} \times \mathbf{H}_0 - \mathbf{n} \times \mathbf{H}_i^N\|_{2,S}}{\|\mathbf{n} \times \mathbf{E}_0\|_{2,S} + \|\mathbf{n} \times \mathbf{H}_0\|_{2,S}} \quad (10)$$

In order to reduce the computational effort, the surface of the scatterer has to be discretized in a set of  $J$  matching points. Thus the integrals appearing in Eq. (9) are approximated by a numerical scheme and the expansion coefficients may formally be written as the solution of the least-squares problem:

$$\mathbf{a} = \arg \min \|\mathbf{A}\mathbf{x} - \mathbf{f}\|_2^2 \quad (11)$$

where the matrix  $\mathbf{A}$  and the vector  $\mathbf{f}$  depend on the values of the spherical vector wavefunctions and the incident field at the matching points, respectively.  $\mathbf{A}$  is a rectangular matrix with the number of matching points  $J$  being larger than the number of multipoles. Equation (11) is solved by using QR decomposition with an algorithm based on Givens rotations.

Because the origin of multipoles can be set very flexible, MMP is able to calculate the field of arbitrarily shaped objects, especially cylinders with large aspect ratios. The drawback of this method is the fairly high computational demands, so that usually only scattering by small cylinders can be calculated with an acceptable error. The size of the fibers presented here is the upper limit for MMP calculation with the IBM RISC 6000 computer that we used. In the future we should be able to calculate even larger objects using the recently developed ‘null-field method with discrete sources’ [15].

#### 4 Results for a $5 \times 1.5 \mu\text{m}$ Fiber

The scattering profiles of several cylinder-shaped fibers with  $5 \mu\text{m}$  length,  $1.5 \mu\text{m}$  diameter and fiber axis orientations of  $45^\circ$  and  $90^\circ$  relative to the axis of the laser beam were simulated using Fraunhofer theory and MMP.

For MMP calculations, the fibers were approximated by 856 matching points (see Figure 2) and 13 poles and the refractive index of refraction was chosen to be from  $1.5-0i$  to  $1.5-1i$ . The real part of the refractive index is in the range of common airborne fibers. Asbestos fibers, for example, have refractive indices ranging from 1.5 to 1.7, depending

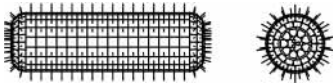


Fig. 2: Fiber shape used for computations in MMP. Left, side view; right, top view. The matching points are shown by its normal vectors. The multipoles were placed along the cylinder axis for the inside field and distributed evenly around the cylinder for the outside field.

on the type of asbestos. The wavelength of the incident beam was chosen to be  $532 \text{ nm}$  in accordance with the wavelength of the laser used by the fiber detector, and the polarization of the beam was parallel to the fiber axis. The resulting scattering profiles are presented in Figure 3 for fiber axis orientation perpendicular and tilted by  $45^\circ$  relative to the axis of the incident laser beam.

For fiber size estimation, the intensity modulations along the vertical and horizontal axes are of interest. The intensity modulations along the vertical axis of the scattering profiles in Figure 3 correspond to the fiber length. The minima positions seem to fit fairly well for the fiber being perpendicular to the laser beam, but some differences of Fraunhofer theory compared with MMP can be observed when looking at the scattering profiles of the tilted fibers. This is due to the three-dimensional fiber geometry, as some light is reflected off the cylinder top, which is not taken into account by Fraunhofer theory.

The intensity modulations along the horizontal axis correspond to the fiber diameter. The minima positions do not fit very well in this case. Looking at the scattering profile of the transparent fiber ( $n_{\text{ref}} = 1.5-0i$ ), the first-order minimum position compared with that of the Fraunhofer fiber seems to be shifted further to higher scattering angles. On the other hand, the diffraction pattern of the Fraunhofer fiber fits fairly well to the scattering profile of the absorbing fibers ( $n_{\text{ref}} = 1.5-0.1i$  and  $n_{\text{ref}} = 1.5-1i$ ), but the position of the second-order minimum does not correspond in this case. Hence there are also differences in minima positions among the profiles of the MMP fibers with different absorption coefficients, so that the scattering profile does seem to depend on the absorption of the fiber material.

For better comparability, the intensity along the vertical and horizontal axes of the scattering profiles are presented in Figure 4 for fiber orientation perpendicular to the laser beam. The deviations in fiber diameter of the two scattering theories were estimated in two different ways. According to Fraunhofer theory the distance of neighboring minima is inversely proportional to the fiber diameter. Thus the error in size estimation can be found directly by analyzing the distance of neighboring minima positions.

The other method looks for the position of the first-order minimum. The minimum position relative to the zeroth-order maximum is also inversely proportional to the fiber diameter. This method is better suited for the estimation of small fiber diameters because the second-order minimum of such fibers is usually difficult to detect because of limited detector apertures.

Looking at the difference in first- and second-order minima positions along the vertical axis of the intensity distributions (corresponding to the fiber length) in Figure 4, good agreement between Fraunhofer and MMP distributions is found. The resulting error in fiber diameter estimation would be less than 10% for both methods. Thus, as

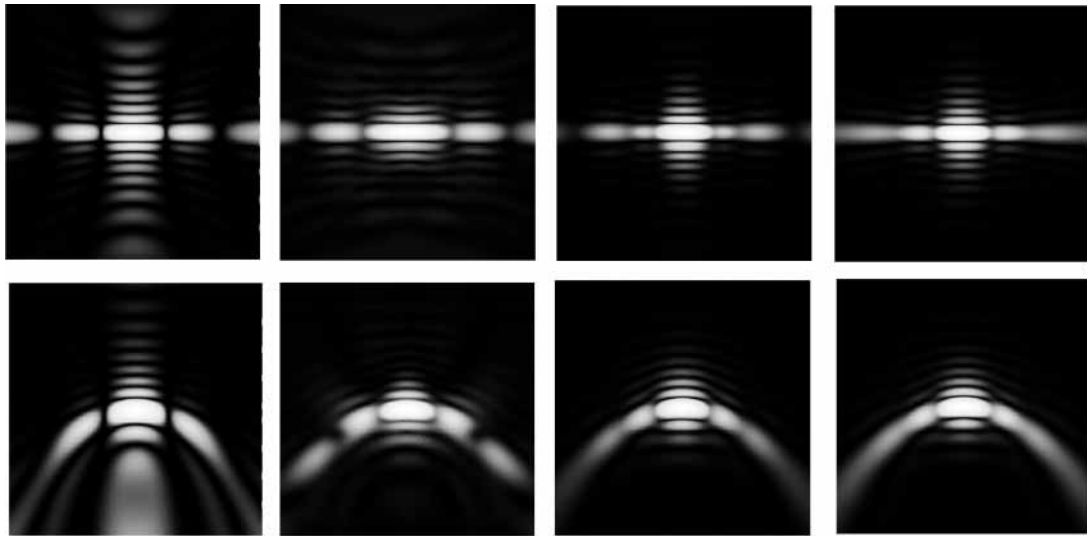


Fig. 3: Simulation of the Fraunhofer profile of a cylindrical fiber (left) compared with the simulations of the scattering profile of the same fiber with MMP having a refractive index of 1.5-0i (middle left), 1.5-0.1i (middle right) and 1.5-1i (right). The fiber geometries are  $5 \times 1.5 \mu\text{m}$ . The fiber axis is orientated perpendicular (center) and tilted by  $45^\circ$  (bottom) relative to the laser beam. The scattering pattern is on a plane at a 50 mm distance from the measurement volume. The plane has a width of  $150 \times 150 \text{ mm}$  corresponding to an aperture angle of  $112^\circ$

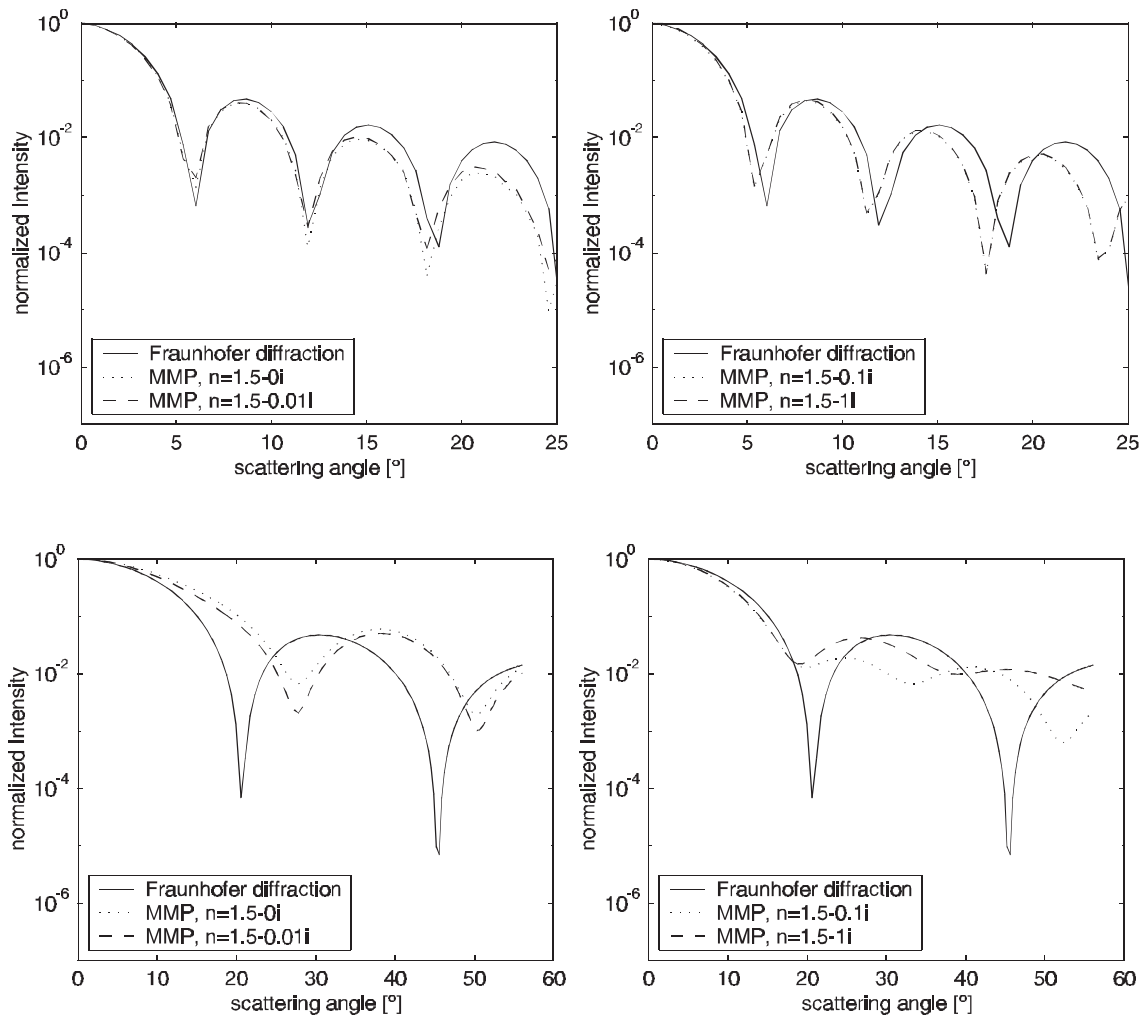


Fig. 4: Vertical (top) and horizontal section (bottom) corresponding to fiber length and diameter of the scattering profiles of the fibers perpendicular to the laser beam in Figure 4, respectively.

expected, Fraunhofer theory gives good results if the geometries are large compared with the wavelength of illumination.

However, for intensity distributions along the horizontal axis in Figure 4 (corresponding to the fiber diameter), differences are found. When estimating the fiber diameter via the first method, the distance between the first- and second-order minima of the Fraunhofer distribution compared with that of the transparent fiber ( $n_{\text{ref}} = 1.5-0i$ ) would lead to an error in diameter of just 5%. For the intensity distributions of the absorbing fibers ( $n_{\text{ref}} = 1.5-0.1i$  and  $n_{\text{ref}} = 1.5-1i$ ), the first and second minima are very close to each other, because there is a secondary maximum at an angle of about  $27^\circ$ . In this case calculation of fiber diameter would lead to an error of about 30% for the highly absorbing fiber ( $n_{\text{ref}} = 1.5-1i$ ) and about 50% for the other absorbing fiber ( $n_{\text{ref}} = 1.5-0.1i$ ), while using the second and third minima of the latter fiber would only lead to an error of 3%.

The second method, which uses the position of the first-order minimum for fiber diameter estimation, leads to different results. According to Figure 4, the first-order minimum position of the Fraunhofer distribution is at a smaller angle than the minima of the intensity distribution of the transparent fiber. The deviation is about 25% for the Fraunhofer fiber when comparing it with the transparent and the lightly absorbing fiber ( $n_{\text{ref}} = 1.5-0.1i$ ), but only about 5% when comparing it with the highly absorbing fibers. Hence in this case fiber diameter estimation of the transparent fiber leads to larger differences.

The reason for the problems in estimating the fiber diameter compared with the fiber length is due to the fact that a diameter of  $1.5 \mu\text{m}$  is only about three times the wavelength of the illuminating laser beam, so that the validity of Fraunhofer theory does not necessarily apply here.

Similar effects can be found for the intensity distributions of fibers tilted by  $45^\circ$ . Furthermore, here only the fiber diameter can be estimated via intensity minima, as the scattering profile along the fiber axis is highly asymmetric because of the fiber tilt. Hence here the fiber length can only be estimated via the half-width of the zeroth-order maximum.

## 5 Results for Various Fiber Diameters

Until now only the scattering profile of one exemplary fiber size has been investigated. Owing to the differences in fiber diameter estimation for the  $5 \times 1.5 \mu\text{m}$  fibers, simulations for several different diameters were done. Scattering profiles of fibers of  $3 \mu\text{m}$  length and diameters from 1 to  $3 \mu\text{m}$  orientated perpendicular to the laser beam were calculated. The length of the fiber was chosen to be short so as to achieve an acceptable computation time. The wavelength of the incident beam was  $532 \text{ nm}$  and the scattering profiles

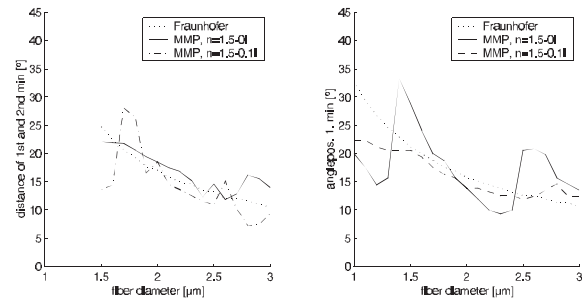


Fig. 5: Distance of the first- and second-order minima for Fraunhofer and MMP simulations (left). Position of the first-order minimum to the zeroth-order maximum (right). The polarization of the  $E$ -vector is parallel to the fiber axis.

were calculated for polarization vectors parallel to the fiber axis.

The intensity distributions along the horizontal axis of the scattering profiles corresponding to various fiber diameters were computed for Fraunhofer theory and MMP. Then the angular minima positions of the distributions were estimated as shown in Figure 5. On the left-hand side the distance between the first- and second-order minima according to the first method are shown for intensity distributions of Fraunhofer and MMP fibers with refractive indices of  $n_{\text{ref}} = 1.5-0i$  and  $n_{\text{ref}} = 1.5-0.1i$ . For fiber diameters smaller than  $1.5 \mu\text{m}$  no calculation can be made for Fraunhofer theory, as it does not give a second-order minimum for an aperture angle restricted to about  $60^\circ$ , which was the maximum aperture angle used for calculations.

Differences due to the distance of neighboring minima are fairly small for fiber diameters larger than  $1.5 \mu\text{m}$  when comparing Fraunhofer intensity distributions with MMP intensity distributions of transparent fibers in Figure 5, but for Fraunhofer and absorbing fiber MMP distributions differences can be found for fiber diameters up to  $2 \mu\text{m}$ . The reason is a local maximum which is present for scattering profiles of absorbing fiber diameters between  $1.25$  and  $1.5 \mu\text{m}$  (see intensity distributions in Figure 6), leading to a smaller distance of the two minima. The algorithm of the detector will spot these minima, resulting in an estimated diameter being too large. At a diameter of  $1.75 \mu\text{m}$  the second-order minimum is shifted to a scattering angle of about  $40^\circ$ , meaning that the diameter will be estimated too small. For diameters larger than  $2 \mu\text{m}$  the absorbing fiber diameter corresponds to that calculated via Fraunhofer theory.

The position of the first-order minimum is presented on the right-hand side of Figure 5. There are only small differences in the minima positions of the Fraunhofer fiber intensity distributions compared with those of absorbing fibers if the fiber diameters are larger than  $1.5 \mu\text{m}$ .

However, looking at the transparent fibers, the first-order minima positions vary significantly. According to Figure 5

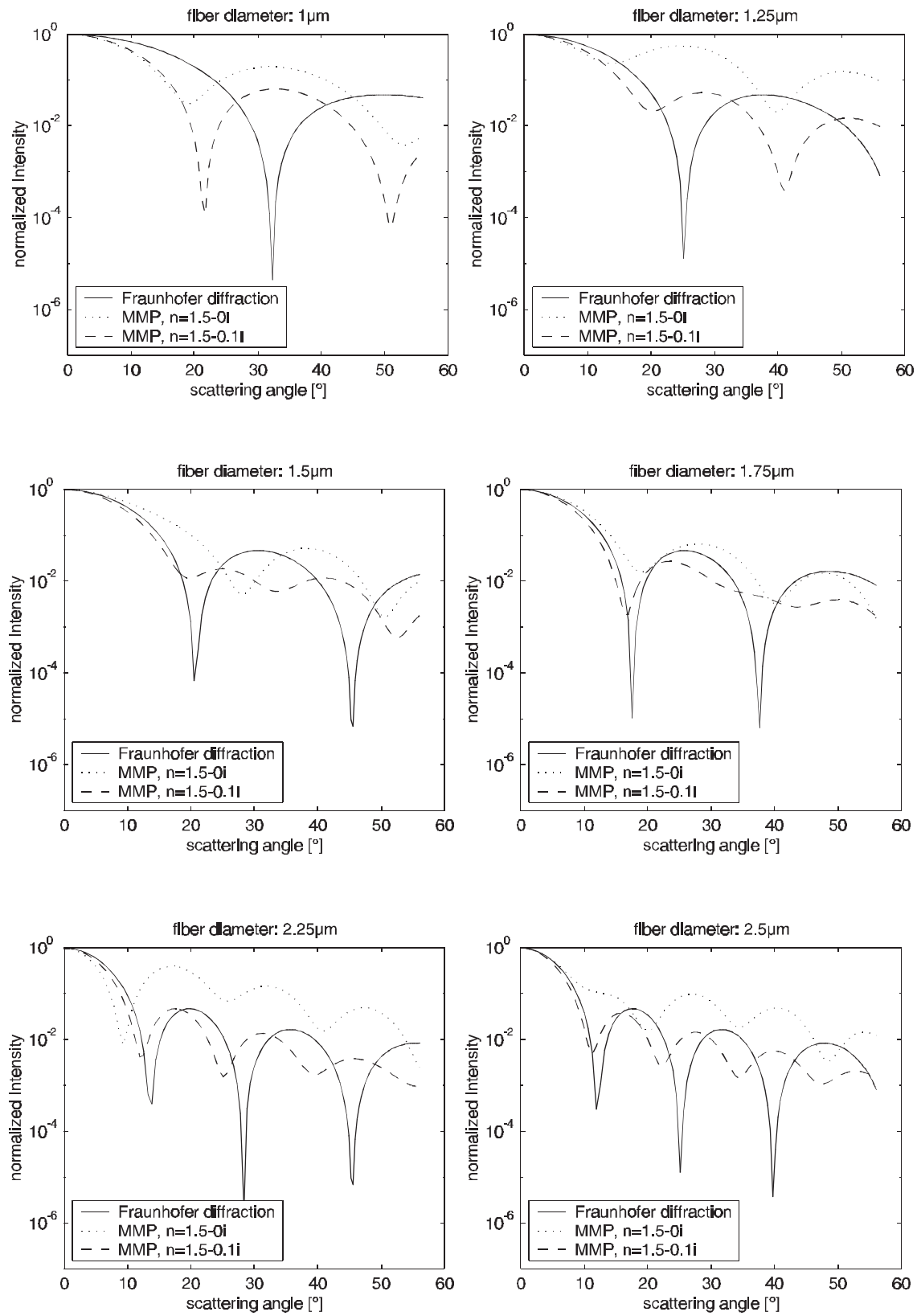


Fig. 6: Intensity distributions corresponding to fiber diameters in the range 1–2.5  $\mu\text{m}$  for Fraunhofer and MMP calculations.

there is no clear relation between fiber diameter in MMP and Fraunhofer distributions. The reason for this is evident when comparing the intensity distributions in Figure 6. The first-order minimum of the scattering profile of the transparent MMP fiber does not correspond to that of the Fraunhofer fiber. The minimum position does not depend at all on the fiber diameter, making fiber size estimation via Fraunhofer theory difficult for small transparent fibers. Similar results were found for polarization of the incident beam perpendicular to the fiber axis.

These deviations may be due to internal effects of light transmitting in the fiber. These internal effects are not taken into account by Fraunhofer theory, where the fiber is assumed to be opaque.

Finally, the results of MMP calculations were validated using the exact solutions of an infinite cylinder with a scattering program developed by Barber and Hill [16]. Calculations were made for various fiber diameters in the range 1–2.5  $\mu\text{m}$ . The results showed excellent agreement with MMP calculations.

## 6 Conclusion

The measurement accuracy of a fiber detector using Fraunhofer theory for determining the size of respirable fibers was investigated using an exact light scattering theory. It was shown that the inaccuracy was about 10% for fiber length determination, which is acceptable because the exact fiber geometries are not of great interest, just the distinction between hazardous and harmless fibers according to the WHO definition.

A different problem is fiber diameter estimation. Here the scattering profile may lead to an error in diameter estimation for thin fibers, which can be up to 60% for a transparent fiber when observing the position of the first minimum only, making fiber size estimation difficult for such fibers. However, the main problem is that the fiber diameter cannot be clearly assigned to the angle of the first-order minimum.

Although the error is fairly large for certain fiber geometries, the overall effect on the number of detected hazardous fibers is small. As the error in fiber diameter estimation only seems to be apparent for fiber diameters of  $\leq 3 \mu\text{m}$ , a fiber being classified as hazardous although being harmless or vice versa only occurs for fibers with lengths of 5–9  $\mu\text{m}$  having also a diameter of  $< 3 \mu\text{m}$  in order to have an aspect ratio of at least 3:1. When estimating fiber concentration in real measurements only a small number of fibers fall into this category. Hence the error in fiber classification will be small compared with the error of the common scanning electron microscopy method.

However, if there is interest in the exact fiber diameter estimation, a calibration function based on Fraunhofer dif-

fraction for large fibers and on MMP for thin fibers has to be used. If fiber diameters of  $< 3 \mu\text{m}$  are investigated, the second-order minimum has to be included in such a calibration curve, as the first-order minimum cannot be clearly assigned to a fiber diameter for transparent fibers. Hence the position of the first-order minimum and the distance of the first and second-order minima have to be used.

## 7 Acknowledgments

The authors thank the Deutsche Forschungsgemeinschaft (DFG) for its support.

## 8 Symbols and Abbreviations

$\mathbf{a}^T = [a_{mnp}^N, b_{mnp}^N, c_{mnp}^N, d_{mnp}^N]$	expansion coefficients
$D_i, D_s$	interior and exterior domain of the dielectric scatterer, respectively
$\mathbf{E}_0, \mathbf{H}_0, \mathbf{E}_i, \mathbf{H}_i, \mathbf{E}_s, \mathbf{H}_s$	electric and magnetic fields of the incident wave, inside the scatterer and of the scattered wave, respectively
$\mathbf{E}_i^N, \mathbf{H}_i^N, \mathbf{E}_s^N, \mathbf{H}_s^N$	approximate solutions of the interior and the scattered fields
$\mathbf{e}_r, \mathbf{e}_\varphi, \mathbf{e}_\theta$	unit vectors in spherical coordinates
$G_i, G_s$	$G_i \subset D_i, G_s \subset D_s$
$h_n$	Hankel function of order $n$
$J$	number of matching points
$j$	imaginary number
$k_0, k_i, k_s$	wavenumber in vacuum, inside the scatterer, of the medium surrounding the scatterer, respectively
$\mathcal{M}_{mnp}^{3t}, \mathcal{N}_{mnp}^{3t}$	radiating spherical vector wave functions
$m$	azimuthal mode
$n$	order of a multipole
$n_{\text{ref}}$	complex index of refraction
$P_n^{ m }$	Legendre polynomial
$S$	boundary of domain $D_i$ (surface of the scatterer)
$x_{0p}$	origin (pole) of a spherical vector wave function

### Greek letters

$\varepsilon_t$	permittivity in domain $D_t$
$\mu_t$	permeability in domain $D_t$

## Subscripts

$i$	field or constant inside the scatterer
$m$	azimuthal mode
$n$	order of the multipole
$p$	number of the multipole
$s$	field or constant of the medium surrounding the scatterer
$t$	$t = s, i$

## 9 References

- [1] *Kommission Reinhaltung der Luft*: Sicherer Umgang mit Fasermaterialien, VDI Berichte 1417. VDI Verlag GmbH, Düsseldorf 1998.
- [2] *German Guideline VDI 3492*: Messen anorganischer faserförmiger Partikel in der Außenluft; Rasterelektronenmikroskopisches Verfahren. Beuth, Berlin 1991.
- [3] *N. Höfert, R. König, K. Grefen, K. Rödelsperger, U. Teichert*: Messen faserförmiger Partikel – Erster Ringversuch nach Richtlinie VDI 3492, Bl. 1, Teil 1 und Teil 2. Gefahrstoffe – Reinhalt. Luft 56 (1996) 11–15, 63–68.
- [4] *N. Höfert, C. Lehmann, M. Sharafi*: Zweiter VDI-Ringversuch “Auswertung von Meßfiltern nach VDI 3492”. Gefahrstoffe – Reinhalt. Luft 59 (1999) 193–197.
- [5] *P. A. Baron*: Direct-reading instruments for aerosols. A review. *Analyst* 119 (1994) 35–40.
- [6] *P. H. Kaye*: Spatial light-scattering analysis as a means of characterizing and classifying nonspherical particles. *Meas. Sci. Technol.* 9 (1998) 141–149.
- [7] *H. Barthel, B. Sachweh, F. Ebert*: Measurement of airborne mineral fibers using a new differential height scattering device. *Meas. Sci. Technol.* 9 (1998) 210–220.
- [8] *J. List, R. Weichert*: Detection of fibers by light diffraction. PARTEC 98, 7th Eur. Symp. Particle Characterization, Nürnberg, Preprints II (1998) 705–714.
- [9] *T. Wriedt*: A Review of Elastic Light Scattering Theories. *Part. Part. Syst. Charact.* 15 (1998) 67–74.
- [10] *H. Barthel*: Ph.D. Thesis, Universität Kaiserslautern, 1999.
- [11] *C. Hafner, K. Bomholt*: The 3D electrodynamic wave simulator. Wiley, Chichester 1993.
- [12] *T. Wriedt*: Generalized multipole techniques for electromagnetic and light scattering. Elsevier, Amsterdam 1999.
- [13] *U. Comberg, T. Wriedt*: Scattering by inhomogeneous particles, exact theories and effective-medium theories, in *T. Wriedt, Y. Eremin* (eds): *Electromagnetic and Light Scattering – Theory and Applications III*. Proc. 3rd Workshop on Electromagnetic and Light Scattering, Bremen 1998, pp. 43–50.
- [14] *T. Wriedt, A. Doicu, U. Comberg, H. Sagehorn, R. Schuh*: Gaussian beam scattering using the discrete sources method, in *G. Gouesbet* (ed): *Scattering of Shaped Light Beams and Applications*. Research Signpost, Trivandrum, India 2000.
- [15] *A. Doicu, Y. Eremin, T. Wriedt*: *Acoustic and Electromagnetic Scattering Analysis Using Discrete Sources*. Academic Press, London 2000.
- [16] *P. W. Barber, S. C. Hill*: *Light Scattering by Particles: Computational Methods*. World Scientific, Singapore 1990.